

GREEN SYNTHESIS AND CHARACTERIZATION OF IRON NANOPARTICLES USING AESCULUS HIPPOCASTANUM SEED EXTRACT

¹DERYA AKSU DEMIREZEN, ²SEYDA YILMAZ, ³DILEK DEMIREZEN YILMAZ

^{1,2}Graduate School of Natural and Applied Sciences, Erciyes University, Kayseri, Turkey

³Biology Department, Faculty of Sciences, Erciyes University, Kayseri, Turkey

^{1,2,3}NanoBiotech, Erciyes Teknopark, Kayseri, Turkey

E-mail: ¹dademirezen@gmail.com, ²seyda.yilmaz100@gmail.com, ³demirezen.dilek@gmail.com

Abstract - Aesculus hippocastanum (horse chestnut) seed extract was used for iron nanoparticles (FeNPs) synthesis in this study. FeNPs were produced and stabilized due to the biomaterials that are found in the content of the seed extract. Particle characterization was analyzed by Transmission electron microscopy (TEM), Energy - dispersive X-ray Spectroscopy (EDX), UV-Visible spectroscopy, Dynamic light scattering (DLS), X-ray diffraction (XRD), Fourier transform infrared spectroscopy (FTIR). Zeta potential and pH were measured. The UV-Visible, XRD, FTIR and analysis results showed that FeNPs were produced in oxide form. Absorption peaks at the wavelength of 205 nm and 291 nm indicated the formation of hydrolysis products of metallic iron (Fe⁰). FTIR, XRD and EDX analysis showed signals due to the oxide and oxyhydroxide iron nanoparticles. TEM images clearly showed that the nanoparticles were in spherical shape mostly with 9 ± 7 nm diameters and were seen as polydisperse. The hydrodynamic diameter of the nanoparticles, that are surrounded by biologic substances adsorbed on the surface, was measured from 50.75 nm to 712.4 nm. Colloid stability was determined as moderate according to 25.5 mV value which was in the range of $\pm 20 - 30$ mV. pH was measured as 6.47 and 2.2 before and after the nanoparticle synthesis respectively.

Keywords - Iron Nanoparticles, Green Synthesis, Green Nanotechnology, Aesculus hippocastanum

I. INTRODUCTION

Nanoparticles that have unique and advanced optical, thermal, electrical, chemical, physical properties are between 1 and 100 nanometers (nm) in size. They are widely used in medicine, chemistry, environment, energy, communication areas [1]. Nanoparticles have been synthesized for a long time by physical and chemical methods but according to recent researches biological (green) synthesis methods provide an alternative way of synthesis due to the rapid, economic and ease of formation of particles. Green synthesis is also an eco-friendly method not using toxic chemicals. In chemical synthesis, chemicals like sodium borohydride or hydrazine hydrate that are used in the production of iron nanoparticles by adsorbing on nanoparticles, lead to raising in toxicity in the environment and harmful effects on living organisms [2].

Biological synthesis of nanoparticles can be carried out with green reagents, microorganisms, plant biomaterials. Green reagents are biopolymers, ascorbic acid, amino acids, hemoglobin etc. Microorganisms are bacteria, fungi, algae. Plant biomaterials are the extracts of leaf, fruit, seed, peel [3]. Plants have the ability to reduce metal ions on their several parts such as leaf, root, tissue, surface and have been used for extracting metals from the ground that is known as phytomining. Interestingly the bioaccumulation studies have shown that metals have been stored as the form of nanoparticles in plants. There are several biomolecules that are playing

role in nanoparticle formation such as terpenoids, polyphenols, sugars. They are responsible for the size and morphology of the synthesized nanoparticles [4]. Using plant extracts making nanoparticles is much more simple, scalable and less expensive method compared to other biological methods. They are responsible for both reducing and stabilizing activities. Different extracts contain different combinations of biomolecules at various concentrations, so the nanoparticles differ. The possible reaction of biochemical constituents with metal ions is seen in Fig. 1 [5].

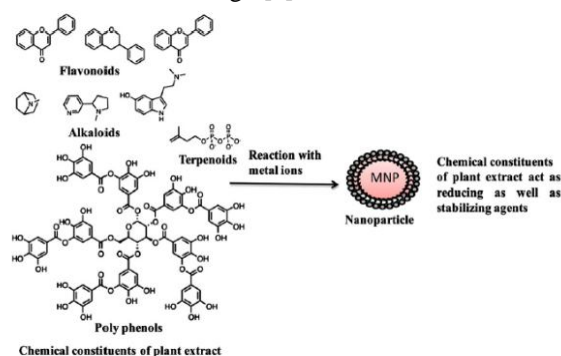


Fig.1. Possible green synthesis of magnetite nanoparticles by plant biochemical molecules

Iron nanoparticles have been used in several areas such as electronic, chemical, environment. It is a strong reductant, so it is widely used in the treatment of toxic chemicals by adsorption or chemical reduction [6]. Due to the decreased particle size, the ratio of atoms to surface area increases. This provides an increase in the adsorption and interactions with the

species (atoms, molecules, complex). Also, they provide advantages like increasing the reaction rate, decreasing reductant dosage and generating nontoxic byproducts [7]. The structure of iron nanoparticles shown in Fig.2 is formed by a zero-valent iron (Fe^0) metallic core and an iron oxide shell. Iron nanoparticles that are larger than 8 nm have the core-shell structure but if the particle is smaller than 8 nm, the overall particle is fully oxidized [8].

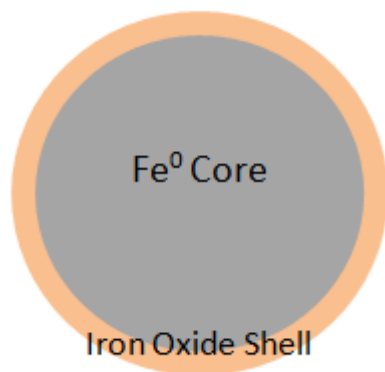


Fig.2. Iron nanoparticle core-shell structure illustration

Aesculus hippocastanum (Horse chestnut) seed contains mainly starch, fat, protein. Besides, there are other biochemical substances such as aescin that is a mixture of saponin glycosides, flavonoids, sterols, essential oil, coumarins and tannins [9]. Starch (carbohydrate) content is mostly found at an average of 34%. It acts as a reducing, stabilizing and dispersant agent in nanoparticle synthesis process. Flavonoids, which belong to polyphenols, are present in a relatively high amount (11.23%) and act as reducing and capping agents [10].

II. DETAILS EXPERIMENTAL

2.1. Materials and Procedures

Aesculus hippocastanum (Horse chestnut) seed was collected at the Erciyes University campus during October 2017 in Kayseri. They were peeled off and dried at room temperature and were cut into small pieces by a plastic knife. Ferric chloride hexahydrate ($\text{FeCl}_3 \cdot 6\text{H}_2\text{O}$) was bought from Merck KGaA, Germany and was used for iron nanoparticle synthesis protocol. Double distilled water was used during the analysis. For the extract preparation; 10 g of horse chestnut seed was weighed and put into 150 ml double distilled water and was boiled at 100°C for 1 hour in a lidded beaker. Seed extract was filtered by Whatman No.1 filter paper and stored in a capped Erlenmeyer flask. 0.14 M ferric chloride solution was prepared by weighing 3.8 g $\text{FeCl}_3 \cdot 6\text{H}_2\text{O}$ and dissolving in 100 ml distilled water. Solution was stirred for 15 minutes.

After extract and ferric chloride solution were prepared, they were mixed at 1:1 volume ratio for nanoparticle synthesis. While adding ferric chloride

solution to extract, continuous stirring of the extract by magnetic stirrer was carried on. Extract color changed from golden to dark brown immediately. That was the indicator of synthesizing iron nanoparticles. The stirring process continued for 2 hours. Prepared nanoparticle solution was stored in liquid form in a capped tube at 4°C . For the powder form of iron nanoparticle preparation; the nanoparticle solution was centrifuged at 4000 rpm during 40 minutes. The liquid part was separated, and the residue was dried at 70°C for 24 hours that was selected according to the literature such as 50°C - 48 hours for leaf extracts [11] and 90°C - 16 hours for banana passion fruit extract [12].

2.2. Characterization of Iron Nanoparticles

Several analyses were made for characterization of iron nanoparticles. Transmission electron microscopy (TEM) analysis was made to indicate the core-shell structure of iron nanoparticles and to measure their size. EDX spectrum analysis was used to see the elemental composition (Fe, O etc.). Hydrodynamic particle size and percentage intensity distribution were measured with Dynamic light scattering (DLS) analysis. Surface charge and colloid stability of the nanoparticles was determined by Zeta Potential (ZP) analysis. X-ray diffraction (XRD) analysis was conducted to investigate the nanoparticle structure such as crystallinity with Bruker AXS D8 advance model. Fourier transform infrared spectroscopy (FTIR) analysis was made by Perkin Elmer Spotlight 400 FTIR microscope to identify the organic and polymeric material. UV absorbance spectra and pH measurement were used to indicate the formation of iron nanoparticles.

III. RESULTS AND DISCUSSION

3.1. FeNPs Synthesis

During the FeNPs synthesis, a sudden color change was observed from golden in Fig.3.a to dark brown in Fig.3.b. This was the first indicator of nanoparticle synthesis as a reduction of ferric (Fe^{+3}) ion. This rapid color change has been seen in several iron nanoparticle synthesis processes in literature at different colors due to the extract phytochemical content such as dark black with nettle leaf extract [13], dark brown with seaweed extract [14], black with eucalyptus leaf extract [15]. pH was measured as 6.47 at the *Aesculus hippocastanum* (Horse chestnut) seed extract and after addition of ferric chloride solution the pH was measured as 2.2. This pH reduction was the second indicator of nanoparticle synthesis in aqueous solution due to the H^+ ion release which is seen at the reaction below. Metallic core of iron nanoparticle is oxidized by water. The products of the corrosion reactions are Fe^{2+} and then Fe^{3+} respectively. Fe^{3+} reacts with water to form iron (III) hydroxide ($\text{Fe}(\text{OH})_3$) and then iron oxyhydroxide (FeOOH) is formed by dehydration. $\text{Fe}(\text{OH})_3$ and

FeOOH precipitate on the iron nanoparticle surface. Single – crystal FeOOH is dehydroxylated to polycrystalline iron oxide (Fe₂O₃) products.[16]

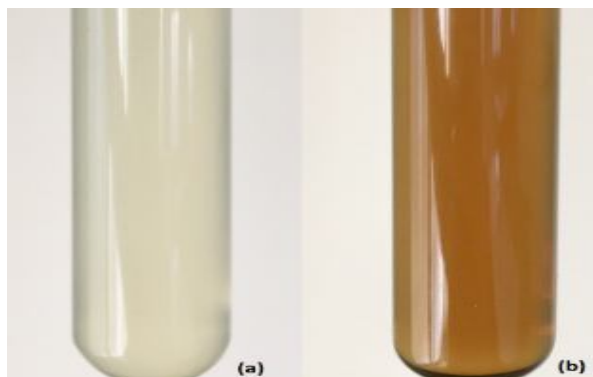
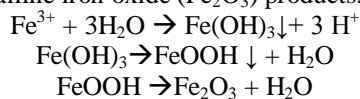


Fig.3. (a) Aesculus hippocastanum (Horse chestnut) seed extract (b) Biologically synthesized iron nanoparticles

3.2. FeNPs Characterization

TEM analysis was used to make morphology (size, shape, distribution) characterization of the nanoparticles. Distribution of the nanoparticles is shown in Fig.4.a. They were synthesized at the oxide form having spherical shapes shown in Fig.4.b. An average size of 9 ± 7 of polydisperse nanoparticles was obtained. Size distribution of the nanoparticles is shown in Fig.5. Starch and flavonoids play important role in reduction, stabilization and uniform distribution of nanoparticles as a capping agent[17].

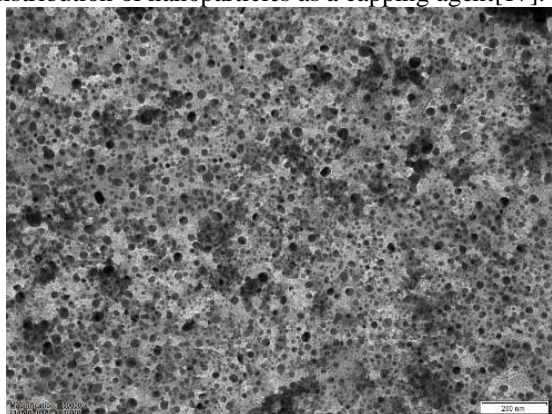


Fig.4.a TEM Image - Distribution of FeNPs

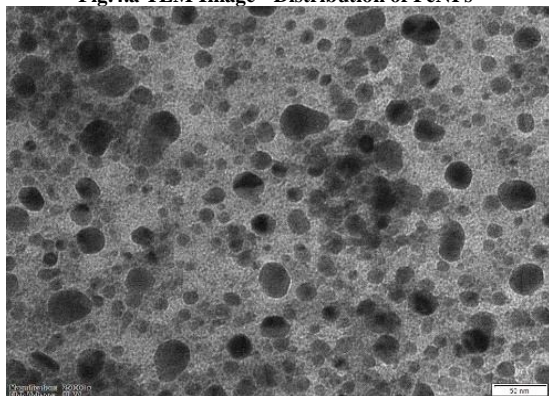


Fig.4.b TEM Image - Shape of FeNPs

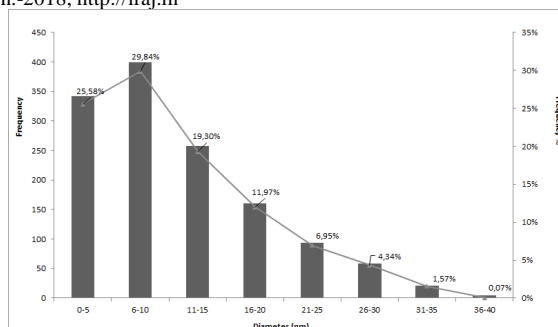


Fig.5. TEM Image – Size Distribution of FeNPs

Percentage of elemental composition was found as 56.18 % oxygen, 12.89 % iron, 30.93 % chlorine by EDX analysis shown in Fig.6. Chlorine signal was originated due to the FeCl₃ that was used in iron synthesis protocol. Oxygen content gives information about the iron oxide forms and was detected at a larger content than the metallic iron. This confirms the formation of iron oxide nanoparticles.

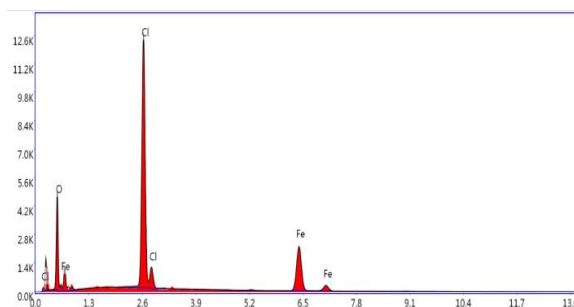


Fig.6. Elemental Composition of Nanoparticles

Hydrodynamic diameter of theoretical sphere of the nanoparticles was measured from 50.75 nm to 712.4 nm shown in Fig.7. This size is the total of metallic core, the biologic substances adsorbed on the surface of the nanoparticles such as stabilizers and the electrical double layer that moves with the particle[18]. The nanoparticles were polydispersed according to the calculated polydispersity index (PDI) measured as bigger than 0.5[19]. The smaller nanoparticles were at high volume percentage according to the intense light scattering from these particles. A little agglomeration occurred due to the clustered nanoparticles.

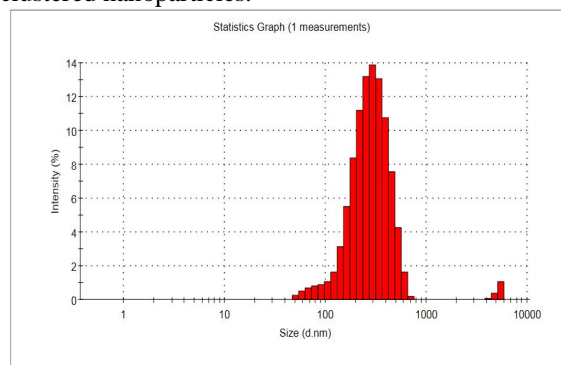


Fig.7. Nanoparticle Hydrodynamic Size Distribution by % Intensity

Zeta Potential (ZP) was measured 25.5 mV at moderate stability. ZP is the relation with the colloid stability and gives indication of it. ZP values of $\pm 0 - 10$ mV (highly unstable), $\pm 10 - 20$ mV (relatively stable), $\pm 20 - 30$ mV (moderately stable), ± 30 mV (highly stable)[20].

The iron (III) hydroxo complex (FeOH^{2+}) hydrolysis product of Fe^0 ; shows maximum absorption spectra at about 300 nm and exactly 205 nm respect to the Cary and Beckman Instruments[21]. After the oxidation of FeOH^{2+} ; FeOOH or $\text{Fe}(\text{OH})_3$ products are generated to form oxide shell of a nanoparticle as a part of the iron nanoparticle synthesis process. Therefore, absorption peaks at 205 nm and 291 nm due to the surface plasmon vibrations that are shown in Fig.8 indicate that nanoparticle hydrolysis process had been occurring[22].

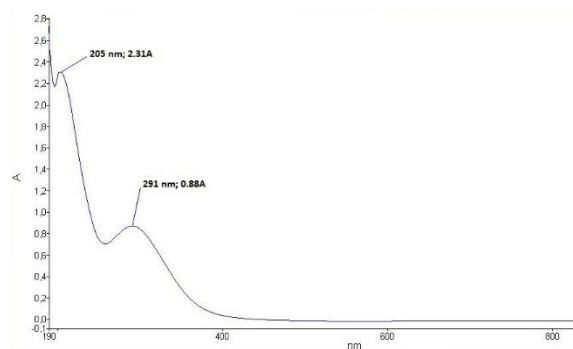


Fig.8. UV Absorption Spectra of Synthesized Nanoparticles

FTIR spectra of iron oxyhydroxide and oxide were shown in Fig.9. The main vibrations of OH groups that are in 2500 to 3800 cm^{-1} regions. These are occurring due to the various iron oxyhydroxides such as $\alpha\text{-FeO}(\text{OH})$ (goethite), $\beta\text{-FeO}(\text{OH})$ (akageneite) and $\gamma\text{-FeO}(\text{OH})$ (lepidocrocite)[23]. The absorption band at lower wavenumber as a result of Fe-O lattice vibration that is given in Table 1. Therefore, adsorption band at 627.5 cm^{-1} refer to Fe-O stretches of maghemite ($\gamma\text{-Fe}_2\text{O}_3$).

Table 1 –Iron Oxides and Infrared Bands [24]

Iron Oxide	Band Wavenumber (cm^{-1})
Magnetite (Fe_3O_4)	400 and 570 (Broad Band)
Maghemite ($\gamma\text{-Fe}_2\text{O}_3$)	620 range, 630-660, 700(Fe-O range)
Hematite ($\alpha\text{-Fe}_2\text{O}_3$)	352, 470, 540

In addition; FTIR spectra provide information about the biomolecule groups in horse chestnut extract. These groups are serving as stabilizing agents on the surface of nanoparticles. Signal at 2084.6 cm^{-1} ($\text{N}=\text{C}=\text{S}$ strong stretching) is due to isocyanate group with a sulfur. The presence of other bands; 1632 cm^{-1} is for C=C medium stretching vibration of conjugated alkene, 1314 cm^{-1} is for O-H medium bending of

phenol, 1163 cm^{-1} is for C-O strong stretching of ester, 993.40 cm^{-1} is for C=C strong bending of alkene [25][26]. All the biomolecule groups act as stabilizers [27][28][29].

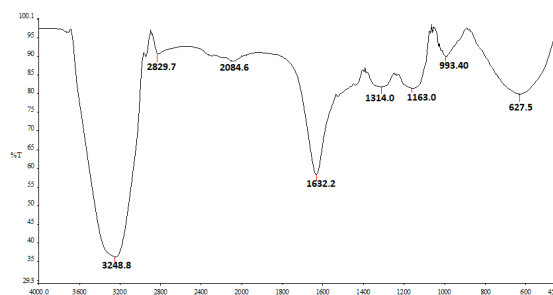


Fig.9. FTIR Spectrum for Synthesized Nanoparticles

The X-ray diffraction (XRD) analysis of the nanoparticle powder were recorded in the range of $2^\circ - 70^\circ$ with step of 0.02° shown in Fig.10. The characteristic peaks were observed at 16° , 20° , 32.5° . These are corresponding to the maghemite ($\gamma\text{-Fe}_2\text{O}_3$) at 32.5° and iron oxyhydroxides ($\gamma\text{-FeO}(\text{OH})$) at 16° and 20° [30].

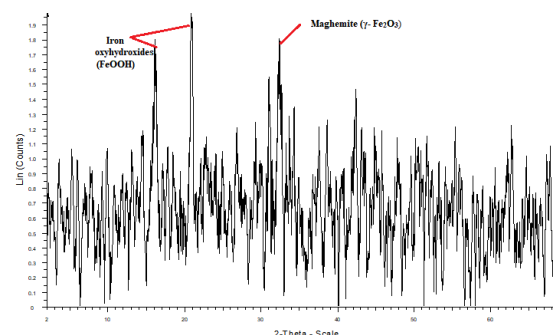


Fig.10. XRD Pattern of Synthesized Nanoparticles

CONCLUSIONS

Iron nanoparticles were synthesized successfully at the average size of 9 ± 7 in a spherical shape by the biochemical agents that are found in the Aesculus hippocastanum (horse chestnut) seed extract. Fe^0 metallic core was oxidized with water so the prepared iron nanoparticles were produced at oxide forms that are suitable for the usage in environmental remediation and biomedical applications.

REFERENCES

- [1] M. Herlekar, S. Bar, and , and R. Kumar, "Plant-Mediated Green Synthesis of Iron Nanoparticles", Journal of Nanoparticles, 2014.
- [2] S. Irvani, "Green synthesis of metal nanoparticles using plants", Green Chemistry, vol. 13, pp. 2638-2650, 2011.
- [3] S. Saif, A. Tahir , and Y. Chen, "Green Synthesis of Iron Nanoparticles and Their Environmental Applications and Implications", Nanometaterials, vol. 6, no. 209, 2016.
- [4] V. V. Makarov, A. J. Lo, and , O. V. Sinititsyna, S. S. Makarova, I. V. Yaminsky, M. E. Taliansky , and N. O. Kalinina, "Green" Nanotechnologies: Synthesis of Metal

- Nanoparticles Using Plants”, *Acta Naturae*, vol. 6, no. 1, pp. 35-4, 2014.
- [5] K. Mittal, Y. Chitti, and U. C. Banerjee, “Synthesis of metallic nanoparticles using plant extracts”, *Biotechnology Advances*, vol. 31, pp. 346-356, 2013.
- [6] J. E. Martin, A. A. Herzing, W. Yan, X.-q. Li, B. E. Koel, C. J. Kiely, and W.-x. Zhang, “Determination of the Oxide Layer Thickness in Core-Shell Zerovalent Iron Nanoparticles”, *Langmuir*, vol. 24, no. 8, pp. 4329-4334, 2008.
- [7] R. Mukherjee, R. Kumar, A. Sinha, Y. Lama, and A. K. Saha, “A review on synthesis characterization and applications of nano zero valent iron (nZVI) for environmental remediation”, *Critical Reviews In Environmental Science and Technology*, vol. 46, no. 5, pp. 443-466, 2016.
- [8] Y. Mu, F. Jia, Z. Ai, and L. Zhang, “Iron oxide shell mediated environmental remediation properties of nano zero-valent iron”, *Environmental Science:Nano*, vol. 4, no. 1, pp. 27-45, 2017.
- [9] Č. Jelena, N.-T. Jelena, L. Mirjana, and K. Aleksandar, “Biochemical composition of the horse chestnut seed (*Aesculus hippocastanum* L.)”, *Biological Sciences*, vol. 63, no. 2, pp. 345-351, 2011.
- [10] G. KSV, H. R. P., and D. Zamare, “Green Synthesis of Iron Nanoparticles Using Green Tea Leaf Extract”, *Journal of Nanomedicine & Biotherapeutic Discovery*, vol. 7, no. 1, pp. 1-4, 2017.
- [11] S. Machado, S.L. Pinto, J.P. Grosso, H. Houws, J.T. Albergaria, and C. Delerue-Matos, “Green production of zero-valent iron nanoparticles using tree leaf extracts”, *Science of the Total Environment*, vol. 445-446, pp. 1-8, 2013.
- [12] B. Kumar, K. Smita, L. Cumbal, and A. Debut, “Biogenic synthesis of iron oxide nanoparticles for 2-arylbenzimidazole fabrication”, *Journal of Saudi Chemical Society*, vol. 18, no. 4, pp. 364-369, 2014.
- [13] Ebrahiminezhad, A. Zare-Hoseinabadi, A. Berenjian, and Y. Ghasemi, “Green synthesis and characterization of zerovalent iron nanoparticles using stinging nettle (*Urtica dioica*) leaf extract”, *Green Processing and Synthesis*, vol. 6, no. 5, pp. 1-7, 2017.
- [14] M. Mahdavi, F. Namvar, M. B. Ahmad, and R. Mohamad, “Green Biosynthesis and Characterization of Magnetic Iron Oxide (Fe₃O₄) Nanoparticles Using Seaweed (*Sargassum muticum*) Aqueous Extract”, *Molecules*, vol. 18, no. 5, pp. 5954-5964, 2013.
- [15] T. Wang, X. Jin, Z. Chen, M. Megharaj, and R. Naidu, “Green synthesis of Fe nanoparticles using eucalyptus leaf extracts for treatment of eutrophic wastewater”, *Science of The Total Environment*, vol. 466-467, no. 1, pp. 210-213, 2014.
- [16] Stefánsson, “Iron(III) Hydrolysis and Solubility at 25 °C”, *Environmental Science and Technology*, vol. 41, no. 17, pp. 6117-6123, 2007.
- [17] V. Veeramanikandan, G.C. Madhu, V. Pavithra, K. Jaianand, and P. Balaji, “Green synthesis, Characterization of Iron Oxide Nanoparticles using *Leucas Aspera* Leaf Extract and Evaluation of Antibacterial and Antioxidant Studies”, *International Journal of Agriculture Innovations and Research*, vol. 6, no. 2, pp. 242-250, 2017.
- [18] E. Tomaszewska, K. Soliwoda, K. Kadziola, B. Tkacz-Szczesna, G. Celichowski, M. Cichomski, W. Szmaja, and J. Grobelny, “Detection limits of DLS and UV-Vis spectroscopy in characterization of polydisperse nanoparticles colloids”, *Journal of Nanomaterials*, vol. 2013, p. 10, 2013.
- [19] M. Nidhin, R. Indumathy, K. J. Sreeram, B. Unni Nair, “Synthesis of iron oxide nanoparticles of narrow size distribution on polysaccharide templates”, *Bulletin of Materials Science*, vol. 31, no. 1, pp. 93-96, 2008.
- [20] S. Bhattacharjee, “DLS and zeta potential – What they are and what they are not?”, *Journal of Controlled Release*, vol. 235, no. 10, pp. 337-351, 2016.
- [21] R. C. Turner, and K. E. Miles, “The Ultraviolet Absorption Spectra of The Ferric Ion and Its First Hydrolysis Product In Aqueous Solutions”, *Canadian Journal of Chemistry*, vol. 35, no. 9, pp. 1002-1009, 1957.
- [22] W. Liang, C. Dai, X. Zhou, and Y. Zhang, “Application of Zero-Valent Iron Nanoparticles for the Removal of Aqueous Zinc Ions under Various Experimental Conditions”, *PLOS ONE*, vol. 9, no. 1, pp. 1-9, 2014.
- [23] S. Ponce-Castañeda, J. Martínez, S. Palomares-Sánchez, F. Ruiz, O. Ayala-Valenzuela, and J. Matutes-Aquino, “Infrared Spectroscopy Analysis of Oxyhydroxides as Intermediate Species in the Formation of Iron Oxides-Silica Xerogels”, *Journal of Sol-Gel Science and Technology*, vol. 27, no. 3, pp. 247-254, 2003.
- [24] H. Namduri, and S. Nasrazadani, “Quantitative analysis of iron oxides using Fourier transform infrared spectrophotometry”, *Corrosion Science*, vol. 50, no. 9, pp. 2493-2497, 2008.
- [25] UCLA, “UCLA”, [Çevrimiçi]. Available: <http://www.ucla.edu>. [Erişildi: 07 February 2018].
- [26] Chemistry LibreTexts, “Chemistry LibreTexts”, [Çevrimiçi]. Available: <https://chem.libretexts.org>. [Erişildi: 07 02 2018].
- [27] B. Ou, D. Li, Q. Liu, Z. Zhou, and B. Liao, “Functionalized TiO₂ nanoparticle containing isocyanate groups”, *Materials Chemistry and Physics*, vol. 135, no. 2-3, pp. 1104-1107, March 2017.
- [28] Ongaro, D. Ryan, and D. Fitzmaurice, “Self-assembly of alkane capped silver and silica nanoparticles”, *Journal of Materials Chemistry*, vol. 12, no. 9, pp. 2762-2768, 2002.
- [29] T. Ahmad, “Reviewing the Tannic Acid Mediated Synthesis of Metal Nanoparticles”, *Journal of Nanotechnology*, vol. 1, pp. 1-11, 2014.
- [30] Liu, J. Liu, B. Pan, and W.-x. Zhang, “Formation of lepidocrocite (γ -FeOOH) from oxidation of nanoscale zerovalent iron (nZVI) in oxygenated water”, *RSC Advances*, vol. 4, no. 101, pp. 57377-57382, 2014.

★★★